Nanoscale

Accepted Manuscript

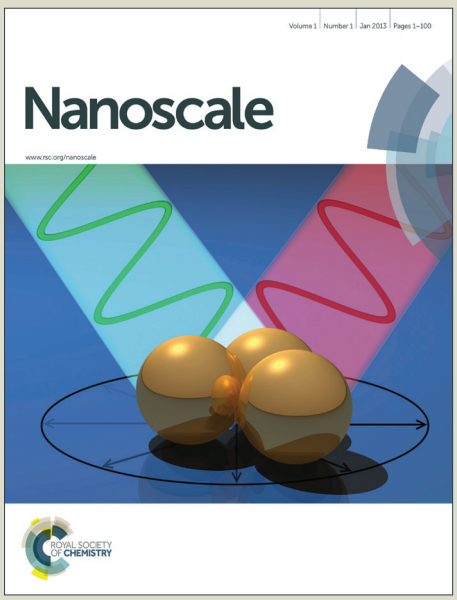

ROYAL SOCIETY OF CHEMISTRY

www.rsc.org/nanoscale

Cite this: DOI: 10.1039/c0xx00000x

www.rsc.org/xxxxxx

ARTICLE TYPE

A novel strategy to synthesize hierarchical porous carbohydrate-derived carbon with tunable properties

Shiping Wang,[a] Ruihan Liu,[b] Chuanlong Han,[a] Jing Wang,[a] Mingming Li,[a] Jia Yao,*[b] Haoran Li[b] and Yong Wang*[a]

Received (in XXX, XXX) Xth XXXXXXXXX 20XX, Accepted Xth XXXXXXXXX 20XX
DOI: 10.1039/b000000x

Hydrothermal carbonization (HTC) of carbohydrate is an interesting candidate for the preparation of carbon materials, as it provides an easy, inexpensive and environmental friendly route. However, it is difficult to prepare porous carbon materials by a straight HTC process. Herein, the solubilising technology of micelles was introduced to direct the HTC of fructose by using an amphiphilic block copolymer, poly-(4-vinylpyridine)-block-poly-(ethylene glycol) (P4VP-PEG), as a structure-directing agent. By this strategy, hierarchical porous carbon materials with tunable properties were prepared. It was investigated that P4VP-PEG micelles could solubilize fructose and confine the formation of primary carbon domains during a sol-gel process. And the micelle size could be adjusted easily by changing the preparation conditions. Accordingly, the particle size of the obtained carbon materials was effectively tuned from 20 to 100 nm by the direction of the primary micelle size. After calcination, the hierarchical porous carbon materials were evidenced as effective electrode materials for supercapacitor with a capacitance of ~197 F at 1 A g^{-1}, which was almost four times higher than the carbon materials prepared by a straight HTC process.

1. Introduction

Carbon materials with high porosity, associated with the advantages of enhanced mass transport and multiple functionalities, are highly desirable and of great potential, in particular for catalysis,[1-5] adsorbent/separation,[6-10] and energy storage/conversion.[11-17] Therefore, many efforts have been made to fabricate porous carbon, and varieties of methods have been developed such as templating method,[18-20] chemical vapor decomposition,[21-24] and chemical or physical activation.[25-27] Considering the energy and sustainability issues, nevertheless, these methods are somewhat fussy, highly costly, and thus unfeasible in industry. Recently, the hydrothermal carbonization (HTC) of carbohydrate has attracted intensive attention for the simple process, the use of environmental friendly aqueous medium and renewable natural resources.[8, 28-35] However, the carbon materials prepared by the straight HTC of carbohydrate are micrometer-sized carbon spheres, which have small specific surface area (<20 m^2 g^{-1}), poor pore structures, and restricted usages.[29, 36-38]

As far, both nanocasting and soft templating strategies have been introduced to the HTC processes. In general, nanocasting strategy employs nanosized porous silica as hard template to introduce pores in the carbonaceous materials.[18, 39-42] Nevertheless, as mentioned above, this nanocasting method is costly, complicated, and always involves the use of highly toxic substances (e.g., NH_4HF_2). Furthermore, the structures and morphologies of the carbon materials synthesized by the nanocasting strategy are limited to the parent silica templates. Meanwhile, it is difficult to obtain porous carbohydrate-derived carbons by soft templating under hydrothermal treatment. The high HTC temperature (160-250 ^oC) might destroy the soft templates (e.g. block copolymer micelles) during the HTC of carbohydrate.[43, 44] Recently, some other efficient techniques have also been developed to synthesize carbon materials with porous structures.[33, 45-53] For example, metal salts, borax or poly-(ionic liquid)s (PILs) additives were used to improve the HTC of carbohydrate and hierarchical porous carbon materials were produced.[28, 46, 49] However, most of the attempts utilize chemicals making the process less green, economic or efficient. Thus, it is still a significant issue to develop novel techniques to improve the HTC processes.

Interestingly, inorganic materials of various structures can be spontaneously fabricated by the direction of colloidal systems. Generally, mesoporous carbon materials are synthesized by

[a] *Carbon Nano Materials Group, Center for Chemistry of High-performance and Novel Materials, Department of Chemistry, Zhejiang University, Hangzhou 310028, P. R. China. E-mail: chemwy@zju.edu.cn*
[b] *State Key Laboratory of Chemical Engineering, Department of Chemistry, Zhejiang University, Hangzhou 310027, P. R. China. E-mail: yaojia@zju.edu.cn*

† Electronic Supplementary Information (ESI) available: [details of any supplementary information available should be included here]. See DOI: 10.1039/b000000x/

nucleation and growth of new forms occurring on the morphological boundary of the colloidal micelles.[19, 54-57] Phenolic resins are the general carbon sources for the preparation of mesoporous carbons by this method. Regarding the economic and ecologic consideration, this method has relatively limited development partly due to the large demand of amphiphilic polymer (the mass ratio of amphiphilic polymer/precursor>0.2), and the fact that harmful phenol and formaldehyde are involved. On the other hand, when the nucleation and growth of new forms are confined within the colloids, refined solid particles are prepared. For instance, carbon spheres were prepared by the Stöber method, which confined the sol-gel process within the emulsions.[58] Regretably, the particle size of carbon spheres was beyond 200 nm because of the limited size of emulsion droplets (usually 0.1 to 10 μm). To control inorganic particles at nanometer-scale, amphiphilic polymer micelles are usually used as structure-directing agents owing to their intrinsic size.[59, 60] By this method, various inorganic nanoparticles such as platinum and gold nanoparticles have been synthesized.[61-63] To the best of our knowledge, there are no reports of the direct synthesis of hierarchical porous carbons by the micelles-assisted method.

Herein, a novel improved HTC of carbohydrate was demonstrated to prepare hierarchical porous carbon materials with tunable properties. Cheap, harmless, and naturally available fructose was employed as a carbon source, and small amount of poly-(4-vinylpyridine)-block-poly-(ethylene glycol) (P4VP-PEG) was used as a structure-directing agent (typically at a P4VP-PEG/ fructose mass ratio of 0.037). By binding onto the blocks of P4VP-PEG, fructose precursors can be solubilized by the micelles, which promoted the formation of primary carbon domains. Based on the sol-gel chemistry, the hierarchical porous carbon materials were prepared. Importantly, this method was simple and effective for the combined control of the textural properties and carbon particle size in a large range from 20 to 100 nm. The hierarchical porous network and short range pores of the obtained carbon materials can provide convenience for interfacial transport, shorten diffusion path or reduce the diffusion effect during diffusion-involved reactions. Indeed, the as-made hierarchical porous carbon materials exhibited commendable capacitance as electrode materials for supercapacitor. The specific capacitance reached to about 197 F at 1 A g^{-1}. In addition, it can be speculated that the obtained hierarchical porous carbon materials have promising potential applications in catalysis, biomedicine and separation for its improved structural properties.

2. Experimental

2.1 Materials and reagents

Fructose (AR), anhydrous alcohol (AR) and polytetra-fluoroethylene (PTFE, 60 wt. %) were purchased from Aladdin and used as received. P4VP-PEG was obtained by a living anionic polymerization,[64] and the preparation process was presented in the supplementary data.

2.2 Hydrothermal synthesis of hierarchical porous carbons

The hierarchical porous carbons were prepared by the HTC of fructose under the direction of amphiphilic diblock copolymer P4VP-PEG. In a typical synthesis, P4VP-PEG and fructose were dissolved in the mixed solvent of 6 mL alcohol and 9 mL water at a P4VP-PEG/fructose mass ratio of 0.037. Subsequently, the mixtures were transferred into a 25 mL Teflon-lined autoclave and kept at 160 ^{o}C for 24 h. The obtained products were rinsed in anhydrous ethanol and deionized water several times and then freeze dried. After that, graphitized carbon materials were obtained by calcining the HTC products at 600 ^{o}C for 4 h and 900 ^{o}C for 1 h in N_2 flow. The resulting hierarchical porous carbons were denoted as HPC-x@y-z, where x and y represented respectively the water/ethanol volume ratio and the P4VP-PEG/fructose mass ratio, z was refer to the pH value of the reaction system. The obtained carbon materials were further used as electrode materials for supercapacitors. The detail preparation parameters of other samples were listed in Table S2.

2.3 Characterization and measurements

The samples were characterized by scanning electron microscopy (SEM), transmission electron microscopy (TEM), N_2 sorption, powder X-ray diffraction (XRD), Raman spectrum, and dynamic light scattering (DLS). SEM analysis was performed on a Hitachi S-4800 electron microscope at an acceleration voltage of 25.0 kV. TEM images were obtained on a Hitachi HT-7700 microscope at 100 kV. ASAP 2020 HD88 surface area and porosity analyzer was used to record the nitrogen adsorption-desorption isotherms. Before the measurement, the samples were dried at 100 ^{o}C for 24 h. The BET specific surface area was determined by a multipoint method. The total pore volume was calculated by the single point adsorption at a relative pressure of 0.98. Besides, the micropore volume was calculated by the V-t plot method and the pore width distributions were obtained by the DFT method. The XRD data were collected using a D/tex-Ultima TV wide angle X-ray diffractionmeter equipped with Cu Kα radiation (1.54 Å), employing a scanning rate of 0.02 s^{-1} at 40 kV and 40 mA. The Raman spectra were measured by a HR-800 Raman spectrometer. Besides, in order to investigate the formation process of the carbon nanoparticles, DLS was carried out with a Malvern Zetasizer Nano ZS instrument.

2.4 Electrochemical evaluation

The sample HPC-1.5@0.077-2 was chosen to prepare supercapacitor for its high surface area. In detail, 9 mg carbon materials were dispersed into 1 mL PTFE anhydrous ethanol solution, 556 μL of which was dropped onto a nickel foam. After air-drying, the carbon casted nickel foam was pressed under 10 MPa for 5 min. The obtained nickel foam was used as the working electrode. Besides, a platinum sheet was used as the counter electrode, and a saturated calomel electrode (SCE) was served as the reference electrode. The cyclic voltammetry was tested on a computer-controlled workstation (LK2005A, China) with a typical three-electrode cell. The galvanostatic charge/discharge behaviors were measured on a battery testing system LAND CT2001A. The specific capacitances were determined from the galvanostatic charge/discharge cycling curves according to the formula: $C = i\Delta t/(mV)$, where i (A) was the current, Δt (s) was the time of discharge, m was the mass (g) of carbon materials casted on the nickel foam and V (V) was the potential.

3. Results and discussion

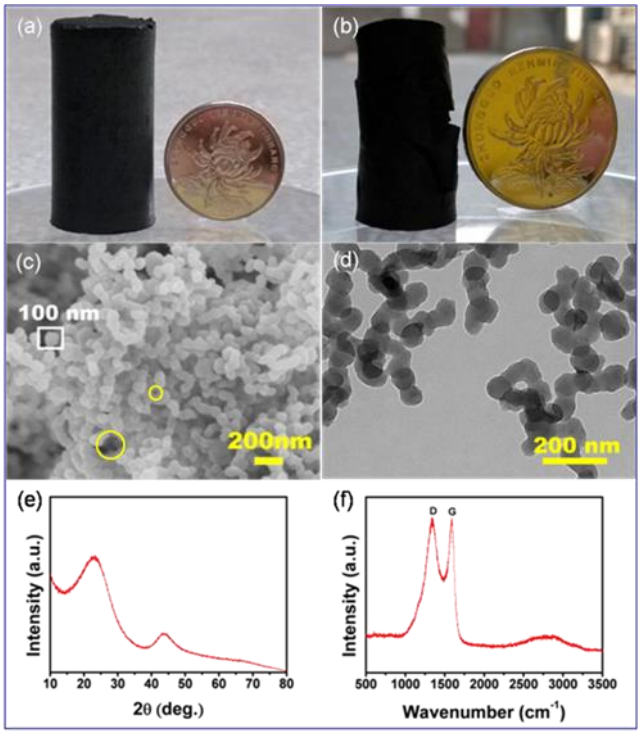

Fig. 1 Characterizations of sample HPC-1.5@0.025-7 prepared under a water/ethanol ratio of 1.5, a P4VP-PEG concentration of 0.01 g mL^{-1} and a fructose concentration of 0.40 g mL^{-1} at pH 7: a) The photo of the HTC carbonaceous materials; b) The photo of the HTC carbonaceous materials after freeze drying and calcination; c) SEM image, the yellow circles highlight the textural meso- and macro-porosities; d) TEM image; e) wide-angle XRD pattern; f) Raman spectrum.

3.1 Structural properties and composition

In this study, hierarchical porous carbons were synthesized by the HTC of fructose under the direction of P4VP-PEG micelles at 160 °C for 24 h with a further calcination process. Representatively, carbogels were synthesized under a water/ethanol volume ratio of 1.5, a P4VP-PEG concentration of 0.01 g mL^{-1} and a fructose concentration of 0.40 g mL^{-1} at pH 7 (HCP-1.5@0.025-7, Table S2, Fig. S2). The photos shown in Fig. 1 a, b revealed the obtained carbogels were mechanically stable with a few contractions after freeze drying and calcination. In contrast with the connected non uniform micrometer-sized spheres prepared from pure fructose solution (Fig. S3 a), the carbon materials prepared from the P4VP-PEG micelles-assisted HTC were hierarchically porous aggregated from nanoparticles with particle size around 100 nm, which was favourable for mass transfer (Fig. 1 c, d). As shown in Fig. S4, macropores ranged from 50 nm to 10 μm were formed in the carbon materials. Besides, the N_2 sorption data confirmed that mesopores and micropores were also existed in the carbon materials (Table 1, Fig. S7 b). As given in Table 1, the total pore volume and micropore volume of sample HPC-1.5@0.025-7 was respectively 0.32 $cm^3\ g^{-1}$ and 0.21 $cm^3\ g^{-1}$. In addition, the wide-angle XRD pattern and Raman spectrum demonstrated the carbogels to be graphitized after calcination (Fig. 1 e, f). The wide-angle XRD pattern showed two main peaks at around 23° and 43.5°, which are the equivalents of the hexagonal graphite 002 (2θ =26°) and 100 (2θ =43°) reflections (Fig. 1 e).[65] The peak shift for the 002 reflection indicated an increase in the interlayer space. This shift might be attributed to the structure defects in the carbon materials.[38, 66] The graphite nature of the obtained carbon materials was also confirmed by the Raman spectrum (Fig. 1 f). The characteristic wide D and G bands at 1340 and 1587 cm^{-1} were related to the breathing mode of aromatic rings and the bond stretching of the sp^2 carbon respectively. This result was consistent with the typical Raman spectra of graphite.[67]

Table 1. N_2 sorption analysis data for the carbon materials obtained by a HTC process under different hydrothermal synthesis parameters with a further calcination at 600 °C for 4 h and 900 °C for 1 h in N_2 flow.

Sample Name	S_{BET}[a] [$m^2\ g^{-1}$]	Pore volume[b] [$cm^3\ g^{-1}$]	Micropore volume[c] [$cm^3\ g^{-1}$]
contrast	447	0.20	0.20
HCP-1.5@0.025-7	510	0.32	0.21
HCP-1.5@0.037-7	562	0.38	0.24
HCP-1.5@0.074-7	553	0.52	0.22
HCP-1.5@0.111-7	535	0.71	0.22
HCP-1.5@0.037-3	543	0.56	0.21
HCP-1.5@0.037-2	571	0.60	0.22
HCP-4@0.037-2	683	0.74	0.26
HCP-0.67@0.037-2	483	0.23	0.21
HCP-1.5@0.077-2	773	0.52	0.32

[a] Brunuaer-Emmett-Teller surface area. [b] Calculated by the single point adsorption at a relative pressure of 0.98. [c] Calculated by the V-t plot method.

3.2 Formation mechanism

The formation mechanism of hierarchical porous materials was proposed as shown in Fig. 2: I) the formation of P4VP-PEG micelles; II) the solubilization of fructose by the micelles; III) the sol-gel process directed by the fructose-solubilized micelles during the HTC; IV) the graphitization of hydrothermal carbon by calcination. Mechanistically, P4VP-PEG amphiphilic block copolymer played a critical role in the formation process.

On the one hand, P4VP-PEG micelles promoted the condensation of fructose and the formation of primary carbon

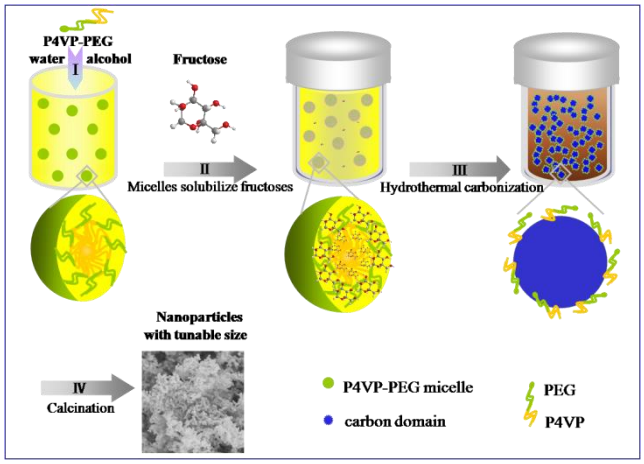

Fig. 2 The mechanism illustration for the formation of hierarchically porous aggregated carbon materials.

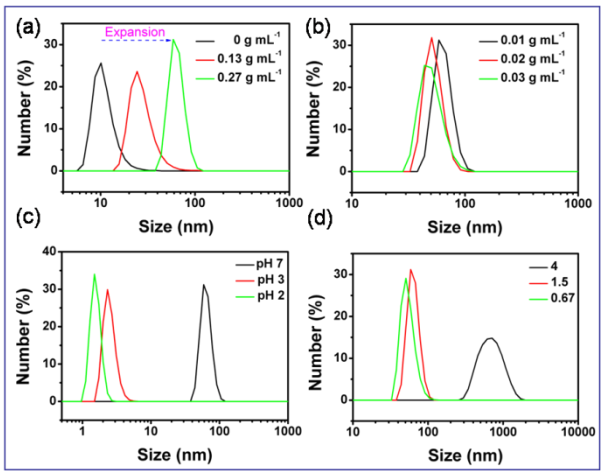

Fig. 3 The size of P4VP-PEG micelles under different preparation parameters: (a) varying fructose concentration under a water/ethanol volume ratio of 1.5 and a P4VP-PEG concentration of 0.01 g mL^{-1} at pH 7; (b) varying P4VP-PEG concentration under a water/ethanol ratio of 1.5 and a fructose concentration of 0.27 g mL^{-1} at pH of 7; (c) varying pH value under a water/ethanol volume ratio of 1.5, a P4VP-PEG concentration of 0.01 g mL^{-1} and a fructose concentration of 0.27 g mL^{-1}; (d) varying water/ethanol volume ratio under a P4VP-PEG concentration of 0.01 g mL^{-1} and a fructose concentration of 0.27 g mL^{-1} at pH 7.

domains during the sol-gel process. As shown in Fig. S5 a, the reaction solution of the contrast sample was clear and yellow when hydrothermal treating for 1 h. However, the reaction solution of sample HPC-1.5@0.037-7, which introduced P4VP-PEG polymers, was muddy with a brown colour under the same hydrothermal conditions (Fig. S5 b). Besides, TEM images showed that there were almost no carbon domains in the reaction system of the contrast sample, while carbon domains formed obviously in the reaction system of sample HPC-1.5@0.037-7 (Fig. S5 a, b). As reported, both P4VP and PEG are hydrophilic blocks, which can form hydrogen bond with the –OH or –NH moieties of the carbon precursors.[19] In this case, fructose molecules could be solubilized in P4VP-PEG micelles by binding onto both blocks of P4VP-PEG. This solubilization process was confirmed by the DLS data to some extent. As shown in Fig. 3 a, without adding fructose, the size of P4VP-PEG micelles was around 10 nm under a water/ethanol volume ratio of 1.5 and a P4VP-PEG concentration of 0.01 g mL^{-1} at pH 7. However, the size increased to 24 nm after the fructose concentration increasing to 0.13 g mL^{-1}. Further increasing the fructose concentration to 0.27 g mL^{-1}, the size sharply increased to 59 nm. Thus, the majority of fructose was confined in the micelles, which resulted in a higher fructose concentration in the micelles than the bulk solution of the contrast sample. Therefore, the condensation rate in the micelles was increased because of the enhanced fructose concentration by the solubilising of micelles.

On the other hand, the P4VP-PEG amphiphilic block copolymer can control the aggregation of the carbon domains and promote the sol-gel process. As shown in the TEM images of Fig. S5 c, carbon domains were formed in the reaction system of the contrast sample after hydrothermal reaction for 3 h. These carbon domains were gradually aggregated into carbonaceous microspheres as increasing the hydrothermal time from 3 to 6 to 24 h (Fig. S5 c, e, g). While in the reaction system of sample HPC-1.5@0.037-7, this aggregation process was inhibited and carbon domains were cross-linked into porous structure based on the sol-gel chemistry (Fig. S5 d, f, h). Furthermore, depositions were observed in the reaction system of the contrast sample after hydrothermal reaction for 3 h and 6 h. As for the sample HPC-1.5@0.037-7, the reaction solution was transformed into sol solution (Fig. S5 d, f). These suggested that the stability of carbon domains in the reaction system of sample HPC-1.5@0.037-7 was much higher than the contrast sample. The enhanced stability of carbon domains should be due to the P4VP-PEG amphiphilic block copolymer on the surface of the carbon domains. Because of the hydrophility of P4VP-PEG polymers, hydrated foam formed on the surface of carbon domains. This improved the intermiscibility of carbon domains in the aqueous solution, and thus the stability of the carbon domains was promoted. Finally, these stabilized carbon domains were slowly growth and cross-linked into gel products as confirmed by Fig. S5 b, d, f, h.

Therefore, it was indicated that the P4VP-PEG micelles could serve as structure directing agents and control the nucleation and growth of carbon domains during the HTC process. Moreover, similar to the conventional silica gels, carbogels were formed by a sol-gel process.[68] Finally, to introduce electric conductivity and improve the stability of the HTC carbonaceous materials, the HTC products were calcined at an elevated temperature. In accordance with the variation of micelle size (Fig. 3 a), the particle size of the hierarchical porous carbons reduced from ~100 (Fig. 1 c, d, HPC-1.5@0.025-7) to ~70 nm (Fig. 4 a, b, HPC-1.5@0.037-7) while decreasing fructose concentration from 0.40 to 0.27 g mL^{-1}.

3.3 Structural control

Interestingly, the textural properties and carbon particle size were tuned by adjusting the preparation parameters (i.e. the P4VP-PEG concentration, the pH of the reaction systems, and the water/ethanol volume ratio) based on the above formation mechanism. Firstly, the effect of P4VP-PEG concentration on the synthesis of carbon materials was investigated while keeping a water/ethanol volume ratio of 1.5 and a fructose concentration of 0.27 g mL^{-1} at pH 7. Typically, as increase the polymer concentration, small organic molecules are more difficult to enter the polymer micelles because of the enhanced micelle stability.[69] On the other hand, the amount of P4VP-PEG micelles increased with the raise of P4VP-PEG concentration. These resulted less fructose molecules solubilization by individual micelles. Consequently, the micelle size decreased from 59 to 51 and then to 44 nm when the P4VP-PEG concentration increased from 0.01 to 0.02 to 0.03 g mL^{-1}(Fig. 3 b). Accordingly, the particle size of the obtained carbon materials, mainly with aggregated porous structures, reduced from ~70 (HPC-1.5@0.037-7, Fig. 4 a, b) to ~65 to ~55 nm (HPC-1.5@0.074-7, HPC-1.5@0.111-7, Fig. S6 a-f). Moreover, the porous structure of the obtained carbon materials was affected by the P4VP-PEG concentration. As given in Table 1, the pore volume increased from 0.38 to 0.52 cm^3 g^{-1} while raising the P4VP-PEG concentration from 0.01 (HPC-1.5@0.037-7) to 0.02 g mL^{-1} (HPC-1.5@0.074-7). By further increasing the P4VP-PEG concentration to 0.03 g mL^{-1} (HPC-1.5@0.111-7), the pore volume reached to 0.71 cm^3 g^{-1}. In addition, the pore width shifted in the range of macropores to

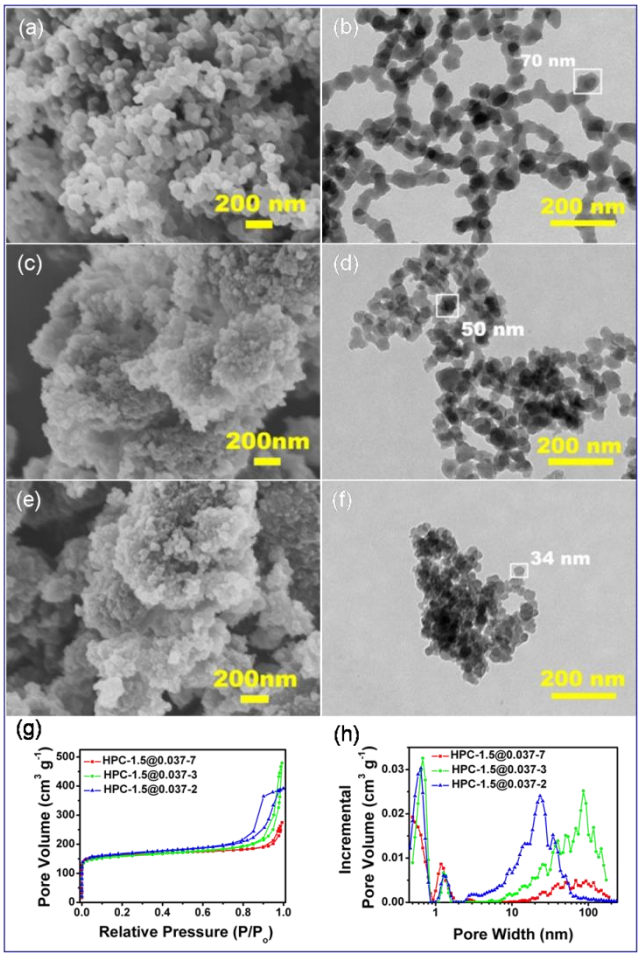

Fig. 4 The SEM and TEM images of the obtained carbon materials prepared under a P4VP-PEG concentration of 0.01 g mL^{-1}, a fructose concentration of 0.27 g mL^{-1} and a water/ethanol ratio of 1.5 at different pH: (a) SEM image of HPC-1.5@0.037-7 prepared at pH 7; (b) TEM image of HPC-1.5@0.037-7; (c) SEM image of HPC-1.5@0.037-3 prepared at pH 3; (d) TEM image of HPC-1.5@0.037-3; (e) SEM image of HPC-1.5@0.037-2 prepared at pH 2; (f) TEM image of HPC-1.5@0.037-2; (g) the N_2 sorption isotherms of the corresponding carbon materials;(h) the pore diameter distributions analyzed by DFT method.

mesopores as confirmed by the pore width distributions (Fig. S7 d, f).

Furthermore, the pH value of the reaction systems had a significant effect on the structural properties and in particularly the particle size of the carbon materials. To investigate the effect of the pH value, the P4VP-PEG concentration and the fructose concentration were respectively kept at 1.5, 0.01 g mL^{-1} and 0.27 g mL^{-1}. The hydrothermal products were unstable gels (pH 3) or sol-like suspensions (pH 2) because of the enhanced electrostatic repulsion (Fig. S2). Commonly, lowering the pH value promoted the protonation of P4VP-PEG polymers, which caused P4VP-PEG micelles to disaggregate.[70] This disaggregation was well evidenced by the DLS measurements. As shown in Fig. 3 c, the micelle size dramatically reduced from 59 to 2.3 to 1.5 nm as decreasing the pH value from 7 to 3 to 2. As a result, the particle size of the carbon materials reduced from ~70 to ~50 to ~34 nm (HPC-1.5@0.037-7, HPC-1.5@0.037-3, HPC-1.5@0.037-2, Fig. 4 a-f). Meanwhile, the porous structures were tuned as demonstrated by the SEM and TEM images (Fig. 4 a-f), which was further confirmed by the N_2 sorption analysis. Fig. 4 g showed a type IV isotherm for sample HPC-1.5@0.037-7. This feature became more evident for sample HPC-1.5@0.037-3 and HPC-1.5@0.037-2 when decreasing the pH value from 7 to 3 to 2. Moreover, the pore diameter distribution graphs (Fig. 4 h) revealed the mesopore diameter reduced as decreasing the pH value. Thus, to some extent, the variation of carbon particle size was in accordance with the variation of mesopore diameter, which implied that the mespores in the obtained carbon materials mainly formed from the stacking of the carbon nanoparticles. Further, an improved specific surface area of 773 m^2 g^{-1} was reached when reducing the fructose concentration to 0.13 g mL^{-1} at pH 2 (HPC-1.5@0.077-2, Table 1, Fig. S8).

The structural properties of the obtained carbon materials can be also tuned by adjusting the water/ethanol volume ratio. As it was reported before, the addition of ethanol increased the solubility of amphiphilic polymer (e.g., P123) and decreased the total volume fraction of polymeric micelles.[71] Similarly, the mixed solution was emulsion when the water/ethanol volume ratio was 4 under a P4VP-PEG concentration of 0.01 g mL^{-1} and a fructose concentration of 0.27 g mL^{-1} at pH 7 (Fig. S9). It turned into transparent solution when the volume ratio decreased to 1.5 and 0.67. And the colloidal particle size decreased from 712 nm to 59 nm and 51 nm (Fig. 3 d). In addition, the addition of ethanol accelerated the fructose-derived oligomers to dissolve and affected the sol-gel process. As a result, the mechanical stability of the obtained carbogels reduced by decreasing the water/ethanol volume ratio (Fig. S2). Correspondingly, the structural properties of the obtained carbon materials were obviously changed. For instance, while decreasing the water/ethanol volume ratio from 4 to 1.5 to 0.67 under a fructose concentration of 0.27 g mL^{-1} and a P4VP-PEG concentration of 0.01 g mL^{-1} at pH 2 (HPC-4@0.037-2, HPC-1.5@0.037-2, HPC-0.67@0.037-2, Table 1), the pore volume reduced from 0.74 to 0.38 to 0.23 cm^3 g^{-1} and the specific surface area decreased from 683 to 562 to 483 m^2 g^{-1}. The obtained carbon materials held the general hierarchical porous structures when the water/ethanol volume ratio was 4 (Fig. S6 g-I, Fig. S7 h). However, it was resulted to be uniform connected structures when the water/ethanol volume ratio was 0.67 (Fig. S6 j-l, Fig. S7 g). Thus, a suitable value of the water/ethanol volume ratio should be adjusted in order to synthesize carbon materials with improved structures.

3.4 Electrochemical evaluation

The obtained carbon materials were evidenced to be effective materials for supercapacitor. Briefly, the electrode of a supercapacitor was prepared by casting the carbon materials onto nickel foam. The electrochemical properties of the casted electrode were evaluated in detail. Here, the sample HPC-1.5@0.077-2 was preferred to be a representative for the relatively great properties (Fig. S8), comparing with the contrast sample. The CV curves of sample HPC-1.5@0.077-2 exhibited a rectangular shape, indicating an ideal double-layer capacitive behaviour (Fig. S10 b). As increase the potential scan rates, the rectangular CV curves were preserved, which revealed the fast charge/discharge behaviour. Moreover, the discharge curves were

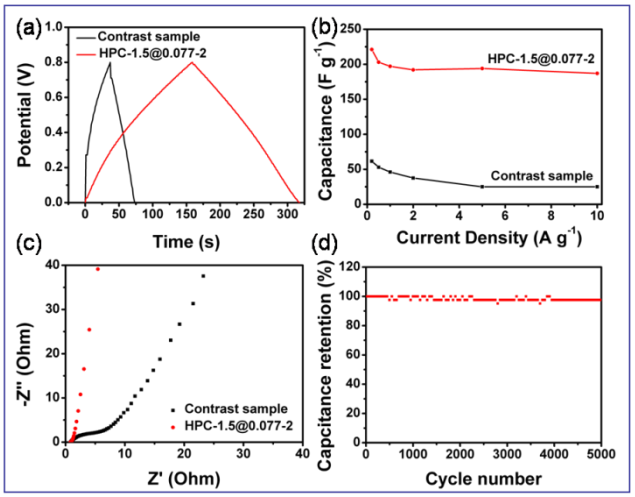

Fig. 5 (a) The galvanostatic charge/discharge graphs of the contrast carbon and sample HPC-1.5@0.077-2 measured at 1 A g^{-1}. (b) The rate capability plots of the contrast sample and sample HPC-1.5@0.077-2 (c) The Nyquist plots of electrochemical impedance of the contrast sample and sample HPC-1.5@0.077-2. (d) The cycling stability of sample HPC-1.5@0.077-2 measured at a current density of 2 A g^{-1}.

symmetric with its corresponding charge curve, suggesting an ideal capacitive behaviour and stable charge/discharge processes (Fig. 5 a, Fig. S10 d). The specific capacitance of the HPC-1.5@0.077-2 casted electrode was calculated to be about 197 F at 1 A g^{-1}, which was about four times higher than the contrast carbon casted electrode (Fig. 5 a). Besides, the capacitances of both the samples were reduced as increasing the current density due to the increasing diffusion limitation (Fig. 5 b). When increasing the current density from 0.2 to 2 A g^{-1}, the capacitance retention of sample HPC-1.5@0.077-2 (87%) was higher than the contrast sample (61%). This improved rate capability can be caused by the hierarchical porous structures and enhanced surface area. Furthermore, the electrochemical impedance spectroscopy (EIS) was also measured at open circuit potential to evaluate the fundamental behaviour of the supercapacitor. The Nyquist plot was given in Fig. 5 c. At very high frequency, the impedance of both samples tended to 0, which was related to the combined resistance of ionic resistance of electrolyte, intrinsic resistance of the carbon materials, and the contact resistance at the interface carbon materials/ nickel foam. At high frequency, the smaller loop of sample HPC-1.5@0.077-2 indicated a lower ions adsorption efficiency and faster ions diffusion/transport, which was due to the hierarchical pores in the carbon materials.[72] At low frequency, the impedance plot of sample HPC-1.5@0.077-2 was more vertical than the contrast carbon, further demonstrating the faster ion diffusion/transport in the electrolyte to the electrode surface of sample HPC-1.5@0.077-2. In addition, the cycling stability of the carbon materials casted electrode was tested at 2 A g^{-1} (Fig. 5 d). After 5000 charge/discharge cycles, about 97 % capacitance was reserved. Therefore, the carbon materials prepared under the direction of P4VP-PEG showed prominently improved electrochemical properties.

4. Conclusions

Hierarchical porous carbons were synthesized by a simple and inexpensive method, which used fructose as the carbon source and introduced P4VP-PEG micelles to direct the formation process. By this method, the particle size of the obtained carbon materials was tuned from 20 to 100 nm, and a highest specific surface area of 773 m^2 g^{-1} was reached. Besides, the formation mechanism was investigated in detail. It indicated that the formation process was controlled through a micelles solubilizing process, which was affected by the preparation parameters including the fructose concentration, the P4VP-PEG concentration, the volume ratio of water/ethanol and the pH value of reaction systems. According to this study, it was an efficient method for large-scale synthesis of carbon materials with particle size less than 100 nm. Furthermore, the obtained carbon materials were used as electrode materials for supercapacitor. A relatively high specific capacitance of ~197 F was reached at 1 A g^{-1}. It can be speculated that by designing the structure of the amphiphilic polymer, nanostructured carbon materials with more special morphologies can be synthesized.

Acknowledgements

Financial support from the National Natural Science Foundation of China (21376208 & U1162124), the Zhejiang Provincial Natural Science Foundation for Distinguished Young Scholars of China (LR13B030001), the Specialized Research Fund for the Doctoral Program of Higher Education (J20130060), the Fundamental Research Funds for the Central Universities, the Program for Zhejiang Leading Team of S&T Innovation, the Partner Group Program of the Zhejiang University and the Max-Planck Society are greatly appreciated.

References

1. S. H. Joo, S. J. Choi, I. Oh, J. Kwak, Z. Liu, O. Terasaki and R. Ryoo, *Nature*, 2001, **412**, 169-172.
2. Z. Sun, B. Sun, M. Qiao, J. Wei, Q. Yue, C. Wang, Y. Deng, S. Kaliaguine and D. Zhao, *J. Am. Chem. Soc.*, 2012, **134**, 17653-17660.
3. C. Han, J. Wang, Y. Gong, X. Xu, H. Li and Y. Wang, *J. Mate. Chem. A*, 2014, **2**, 605-609.
4. J. Guerra and M. A. Herrero, *Nanoscale*, 2010, **2**, 1390-1400.
5. X. Xu, M. Tang, M. Li, H. Li and Y. Wang, *ACS Catalysis*, 2014, **4**, 3132-3135.
6. C. Liang, S. Dai and G. Guiochon, *Anal. Chem.*, 2003, **75**, 4904-4912.
7. W. Yantasee, Y. H. Lin, G. E. Fryxell, K. L. Alford, B. J. Busche and C. D. Johnson, *Ind. Eng. Chem. Res.*, 2004, **43**, 2759-2764
8. R. J. White, C. Antonio, V. L. Budarin, E. Bergström, J. Thomas-Oates and J. H. Clark, *Adv. Funct. Mater.*, 2010, **20**, 1834-1841.
9. M. Sevilla and A. B. Fuertes, *Energy Environ. Sci.*, 2011, **4**, 1765-1771.
10. Z. Sun, Y. Liu, B. Li, J. Wei, M. Wang, Q. Yue, Y. Deng, S. Kaliaguine and D. Zhao, *Acs. Nano.*, 2013, **7**, 8706-8714
11. J. Lee, S. Yoon, T. Hyeon, S. M. Oh and K. B. Kim, *Chem. Commun.*, 1999, 2177-2178.
12. Y. S. Hu, P. Adelhelm, B. M. Smarsly, S. Hore, M. Antonietti and J. Maier, *Adv. Funct. Mater.*, 2007, **17**, 1873-1878.
13. P. Simon and Y. Gogotsi, *Nat. Materials*, 2008, **7**, 845-854
14. H. Zhu, X. Wang, F. Yang and X. Yang, *Adv. Mater.*, 2011, **23**, 2745-2748.
15. Y. Cheng, S. Lu, H. Zhang, C. V. Varanasi and J. Liu, *Nano Lett.*, 2012, **12**, 4206-4211.
16. Z. Yan, L. Ma, Y. Zhu, I. Lahiri, M. G. Hahm, Z. Liu, S. Yang, C. Xiang, W. Lu, Z. Peng, Z. Sun, C. Kittrell, J. Lou, W. Choi, P. M. Ajayan and J. M. Tour, *ACS Nano*, 2012, **7**, 58-64.
17. S. Liu, S. Sun and X. Z. You, *Nanoscale*, 2014, **6**, 2037-2045.

18. C. Liang, Z. Li and S. Dai, *Angew. Chem. Int. Ed.*, 2008, **47**, 3696-3717.
19. L. Chuenchom, R. Kraehnert and B. M. Smarsly, *Soft Matter.*, 2012, **8**, 10801-10812.
20. Y. Deng, J. Wei, Z. Sun and D. Zhao, *Chem. Soc. Rev.*, 2013, **42**, 4054-4070.
21. A. Eftekhari, P. Jafarkhani and F. Moztarzadeh, *Carbon*, 2006, **44**, 1343-1345.
22. L. Mleczko and G. Lolli, *Angew. Chem. Int. Ed.*, 2013, **52**, 9372-9387.
23. A. Baliyan, Y. Nakajima, T. Fukuda, T. Uchida, T. Hanajiri and T. Maekawa, *J. Am. Chem. Soc.*, 2014, **136**, 1047-1053.
24. C. Qian, H. Qi and J. Liu, *J. Phys. Chem. C*, 2007, **111**, 131-133.
25. F. Rodríguez-Reinoso, M. Molina-Sabio and M. T. González, *Carbon*, 1995, **33**, 15-23.
26. A. M. Puziy, O. I. Poddubnaya, A. Martínez-Alonso, F. Suárez-García and J. M. D. Tascón, *Carbon*, 2003, **41**, 1181-1191.
27. L. Zhang, X. Yang, F. Zhang, G. Long, T. Zhang, K. Leng, Y. Zhang, Y. Huang, Y. Ma, M. Zhang and Y. Chen, *J. Am. Chem. Soc.*, 2013, **135**, 5921-5929.
28. X. Cui, M. Antonietti and S. H. Yu, *Small*, 2006, **2**, 756-759.
29. M. Sevilla and A. B. Fuertes, *Carbon*, 2009, **47**, 2281-2289.
30. R. J. White, V. Budarin, R. Luque, J. H. Clark and D. J. Macquarrie, *Chem. Soc. Rev.*, 2009, **38**, 3401-3418.
31. D. Jagadeesan and M. Eswaramoorthy, *Chem. Asian J.*, 2010, **5**, 232-243.
32. L. Zhao, N. Baccile, S. Gross, Y. Zhang, W. Wei, Y. Sun, M. Antonietti and M.-M. Titirici, *Carbon*, 2010, **48**, 3778-3787.
33. H. W. Liang, Q. F. Guan, L. F. Chen, Z. Zhu, W. J. Zhang and S. H. Yu, *Angew. Chem. Int. Ed.*, 2012, **51**, 5101-5105.
34. N. Fechler, S.-A. Wohlgemuth, P. Jäker and M. Antonietti, *J. Mater. Chem. A*, 2013, **1**, 9418-9421.
35. C. Han, S. Wang, J. Wang, M. Li, J. Deng, H. Li and Y. Wang, *Nano Research*, 2014, DOI: 10.1007/s12274-014-0540-x.
36. M.-M. Titirici, M. Antonietti and N. Baccile, *Green Chem.*, 2008, **10**, 1204-1212.
37. J. Ryu, Y.-W. Suh, D. J. Suh and D. J. Ahn, *Carbon*, 2010, **48**, 1990-1998.
38. L. Yu, C. Falco, J. Weber, R. J. White, J. Y. Howe and M.-M. Titirici, *Langmuir*, 2012, **28**, 12373-12383.
39. A. Lu, A. Kiefer, W. Schmidt, F. Schüth, *Chem. Mater.*, 2004, **16**, 100-103.
40. J. Lee, J. Kim and T. Hyeon, *Adv. Mater.*, 2006, **18**, 2073-2094.
41. S. Kubo, R. Demir-Cakan, L. Zhao, R. J. White and M. M. Titirici, *ChemSusChem*, 2010, **3**, 188-194.
42. L. Yu, N. Brun, K. Sakaushi, J. Eckert and M.-M. Titirici, *Carbon*, 2013, **61**, 245-253.
43. P. Bloss, W.-D. Hergeth, E. Döring, K. Witkowski and S. Wartewig , *Acta Polym.*, 1989, **40**, 260-265.
44. S. Kubo, R. J. White, N. Yoshizawa, M. Antonietti and M.-M. Titirici, *Chem. Mater.*, 2011, **23**, 4882-4885.
45. S.-A. Wohlgemuth, R. J. White, M.-G. Willinger, M.-M. Titirici and M. Antonietti, *Green Chem.*, 2012, **14**, 1515-1523.
46. T.-P. Fellinger, R. J. White, M.-M. Titirici and M. Antonietti, *Adv. Funct. Mater.*, 2012, **22**, 3254-3260.
47. N. Brun, C. A. García-González, I. Smirnova and M.-M. Titirici, *RSC Adv.*, 2013, **3**, 17088-17096.
48. N. Brun, S. A. Wohlgemuth, P. Osiceanu and M.-M. Titirici, *Green Chem.*, 2013, **15**, 2514-2524.
49. P. Zhang, J. Yuan, T. P. Fellinger, M. Antonietti, H. Li and Y. Wang, *Angew. Chem. Int. Ed.*, 2013, **52**, 6028-6032.
50. Z.-L. Xie, R. J. White, J. Weber, A. Taubert and M.-M. Titirici, *J. Mater. Chem.*, 2011, **21**, 7434-7442.
51. M. Antonietti, N. Fechler and T.-P. Fellinger, *Chem. Mater.*, 2014, **26**, 196-210.
52. P. Zhang, Y. Gong, Z. Wei, J. Wang, Z. Zhang, H. Li, S. Dai and Y. Wang, *ACS Appl. Mater. Interfaces*, 2014, **6**, 12515-12522.
53. Y. Gong, L. Xie, H. Li and Y. Wang, Chem. Commun., 2014, DOI: 10.1039/C4CC04998E.
54. J. Xue, G. Singh, Z. Qiang, A. Karim and B. D. Vogt, *Nanoscale*, 2013, **5**, 7928-7935.
55. Y. Deng, T. Yu, Y. Wan, Y. Shi, Y. Meng, D. Gu, L. Zhang, Y. Huang, C. Liu, X. Wu and D. Zhao, *J. Am. Chem. Soc.*, 2007, **129**, 1690-1697.
56. C. Liang and S. Dai, *J. Am. Chem. Soc.*, 2008, **128**, 5316-5317.
57. Y. Fang, D. Gu, Y. Zou, Z. Wu, F. Li, R. Che, Y. Deng, B. Tu and D. Zhao, *Angew. Chem. Int. Ed.*, 2010, **49**, 7987-7991.
58. J. Liu, S. Z. Qiao, H. Liu, J. Chen, A. Orpe, D. Zhao and G. Q. Lu, *Angew. Chem. Int. Ed.*, 2011, **50**, 5947-5951.
59. Z. Sun, F. Bai, H. Wu, S. K. Schmitt, D. M. Boye, Z. Jiang, J. Wang and H. Fan, *Chem. Eur. J.*, 2009, **15**, 11128-11133.
60. R. Muñoz-Espí, Y. Mastai, S. Gross and K. Landfester, *CrystEngComm*, 2013, **15**, 2175-2191.
61. A. Kohut, A. Voronov, V. Samaryk and W. Peukert, *Macromol. Rapid Commun.*, 2007, **28**, 1410-1414.
62. N. Hoda, L. Budama, B. A. Çakır, Ö. Topel and R. Ozisik, *Mater. Res. Bull.*, 2013, **48**, 3183-3188.
63. L. Yu, J.-J. Qiu, H. Cheng and Z.-H. Luo, *Mater. Chem. Phys.*, 2013, **138**, 780-786.
64. M. Szwarc, *Nature*, 1956, **178**, 1168-1169
65. Z. Q. Li, C. J. Lu, Z. P. Xia, Y. Zhou and Z. Luo, *Carbon*, 2007, **45**, 1686-1695.
66. S.-A. Wohlgemuth, F. Vilela, M.-M. Titirici and M. Antonietti, *Green Chemistry*, 2012, **14**, 741-749.
67. G. Eda and M. Chhowalla, *Adv. Mater.*, 2010, **22**, 2392-2415.
68. K. Nakanishi, *J. Porus Mater.*, 1997, **4**, 67-112.
69. G. Ma, X. Yan, Y. Li, L. Xiao, Z. Huang, Y. Lu and J. Fan, *J. Am. Chem. Soc.*, 2010, **132**, 9596-9597.
70. J. Yao, H. Wu, Y. Ruan, J. Guan, A. Wang and H. Li, *Polymer*, 2011, **52**, 793-803.
71. J. S. Lettow, T. M. Lancaster, C. J. Glinka and J. Y. Ying, *Langmuir*, 2005, **21**, 5738-5746.
72. J. Gamby, P. L. Taberna, P. Simon, J. F. Fauvarque and M. Chesneau, J. Power Sources, 2001, **101**, 109-116.